

# Improvement of fatigue resistance of epoxy composite with microencapsulated epoxy-SbF<sub>5</sub> self-healing system

X. J. Ye<sup>1,2</sup>, Y. Zhu<sup>2</sup>, Y. C. Yuan<sup>3</sup>, Y. X. Song<sup>2</sup>, G. C. Yang<sup>2</sup>, M. Z. Rong<sup>2</sup>, M. Q. Zhang<sup>2\*</sup>

<sup>1</sup>Guangdong Provincial Public Laboratory of Analysis and Testing Technology, China National Analytical Center, 510070 Guangzhou, P. R. China

<sup>2</sup>Key Laboratory for Polymeric Composite and Functional Materials of Ministry of Education, GD HPPC Lab, School of Chemistry, Sun Yat-Sen University, 510275 Guangzhou, P. R. China

<sup>3</sup>College of Materials Science and Engineering, South China University of Technology, 510640 Guangzhou, P. R. China

Received 29 March 2017; accepted in revised form 21 May 2017

**Abstract.** Rapid retardation and arresting of fatigue crack are successfully realized in the epoxy composite containing microencapsulated epoxy and ethanol solution of antimony pentafluoride-ethanol complex (SbF<sub>5</sub>·HOC<sub>2</sub>H<sub>5</sub>/HOC<sub>2</sub>H<sub>5</sub>). The effects of (i) microcapsules induced-toughening, (ii) hydrodynamic pressure crack tip shielding offered by the released healing agent, and (iii) polymeric wedge and adhesive bonding of cured healing agent account for extension of fatigue life of the material. The two components of the healing agent can quickly react with each other soon after rupture of the microcapsules, and reconnect the crack only 20 seconds as of the test. The applied stress intensity range not only affects the healing efficiency, but also can be used to evaluate the healing speed. The present work offers a very fast healing system, and sets up a framework for characterizing speed of self-healing.

**Keywords:** smart polymers, fracture and fatigue, self-healing, epoxy

## 1. Introduction

Self-healing has been regarded as an important and smart measure to improve stability and durability of polymeric materials [1–3]. More and more researchers started to study this topic because of its scientific and technical merits. In addition to the degree of properties restoration enabled by self-healing, healing speed has attracted increasing research interests because cracks should be eliminated as soon as they are initiated [4]. It is critical for practice application to prevent catastrophic failure, especially for the products in service. There are two healing strategies available for polymers and polymer composites, i.e. intrinsic and extrinsic self-healing. The former operates through reversible inter- and/or intra-macromolecular interaction (like hydrogen bond [5],  $\pi$ - $\pi$  stacking [6], ionic interaction [7], host-guest interaction [8], metal-ligand

coordination [9], imine bond [10, 11], Diels-Alder bond [12], disulfide bond [13], C–ON bond [14], coumarin derivatives [15], and boronic ester linkages [16]), while the latter relies on the embedded healing agent (mostly fluidic) stored in microcapsules [17, 18] or microtubes [19, 20]. Compared to intrinsic self-healing, extrinsic self-healing is able to burst out fluidic healing agent upon cracking so that it is in a better position to realize high speed rehabilitation [21–26]. On the basis of this consideration, a few fast healing chemistries and the related healing systems were successively explored in our laboratory [27–33]. Cationic chain polymerization of epoxy monomers catalyzed by antimony pentafluoride [29, 30], for example, proved to heal cracks within seconds. To further examine the fast self-healability of the system in authentic specimen, fatigue performance

\*Corresponding author, e-mail: [ceszmq@mail.sysu.edu.cn](mailto:ceszmq@mail.sysu.edu.cn)  
© BME-PT

of epoxy composite containing dual capsules, i.e. epoxy monomer-loaded microcapsules and ethanol solution of antimony pentafluoride-ethanol complex ( $\text{SbF}_5 \cdot \text{HOC}_2\text{H}_5/\text{HOC}_2\text{H}_5$ )-loaded microcapsules, is investigated in the present work. It is known that the competition between chemical kinetics of healing agents and mechanical kinetics of crack propagation determines the extent of fatigue life extension [34, 35]. In other words, retardation or arresting of fatigue crack is rather sensitive to the polymerization rate of healing agent. Therefore, the effect of fatigue crack induced liberation of healing agent can be conveniently monitored by mechanical response of the composite, i.e. *in-situ* crack re-binding and growth under cyclic stress. In contrast, other destructive characterization methods, like tensile [15] and impact tests [24, 27], need time for manually recombining the fractured specimens for healing and quite a few fast healing agent would have been cured in advance. The measured dependence of healing efficiency on healing time has to be associated with large error. So far, fatigue resistance of self-healing polymers and polymer composites has not been extensively studied. Moreover, healing speed is not the main concern of these available works [35–43]. In this context, the present investigation might add to the researches in this area.

## 2. Experimental

### 2.1. Materials

Diglycidyl ether of bisphenol A (EPON 828, epoxy value: 0.53~0.54 mol/100 g), supplied by Shell Co., served as the composite's matrix and the polymerizable component of healing system. Antimony pentafluoride ( $\text{SbF}_5$ ) was purchased from Tianjin Institute of Physical and Chemical Engineering of Nuclear Industry, China. Borontrifluoride-2,4-dimethylaniline-complex ( $\text{BF}_3 \cdot \text{DMA}$ ) and methyl hexahydrophthalic anhydride (MHHPA) were bought from Energy Chemical, Shanghai, China. Ethanol, tetraethyl orthosilicate (TEOS), styrene and methyl acrylate were supplied by Alfa Aesar GmbH, Germany. Prior to use, styrene and methyl acrylate were washed with sodium hydroxide aqueous solution (5 wt%), thereafter three times with water, dried over magnesium sulphate, and evaporated to dryness in vacuum. Azobisisobutyronitrile (AIBN) was obtained from Sigma-Aldrich, and purified by recrystallization.

Melamine and formaldehyde were supplied by Sinopharm Chemical Reagent Co., Ltd, Shanghai, China.

### 2.2. Specimens preparation

Epoxy monomer was encapsulated by poly(melamine formaldehyde) (PMF) as described in ref. [44]. The average diameter and core content of the resultant spheres are 130  $\mu\text{m}$  and 91 wt%, respectively.

Ethanol solution of antimony pentafluoride-ethanol complex ( $\text{SbF}_5 \cdot \text{HOC}_2\text{H}_5/\text{HOC}_2\text{H}_5$ ) was prepared by the method mentioned in ref. [45] to reduce the high reactivity of  $\text{SbF}_5$  for easy handling. Next, silica walled microcapsules containing  $\text{SbF}_5 \cdot \text{HOC}_2\text{H}_5/\text{HOC}_2\text{H}_5$  were prepared by vacuum aided infiltration [28]. The average diameter and core content of these hardener-loaded microcapsules are 6  $\mu\text{m}$  and about 40 wt%, respectively.

Unfilled tapered double cantilever beam (TDCB) specimens (with groove length of 55 mm [46], Figure 1) were cast from the stoichiometric mixture of accelerant  $\text{BF}_3 \cdot \text{DMA}$  (5 parts), curing agent MHHPA (80 parts) and epoxy EPON 828 (100 parts). Meanwhile, the self-healing TDCB specimens were prepared by uniformly compounding epoxy-loaded microcapsules and  $\text{SbF}_5 \cdot \text{HOC}_2\text{H}_5/\text{HOC}_2\text{H}_5$ -loaded microcapsules with the aforesaid mixture of  $\text{BF}_3 \cdot \text{DMA}$ , MHHPA and EPON 828. The compounds were degassed, poured into a preheated closed silicone rubber mold, and cured at 50 °C for 60 h and 70 °C for 12 h. Unless otherwise specified, the contents of the epoxy monomer- and hardener-loaded microcapsules were 10 and 0.6 wt%, respectively. The control composite specimen has the same composition as the self-healing one except that the hardener capsules were replaced by ethanol capsules.

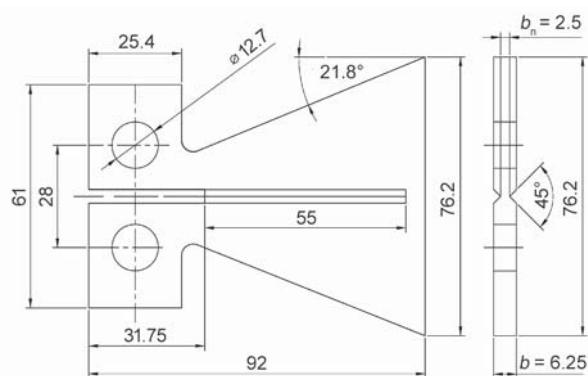


**Figure 1.** TDCB geometry with 55 mm side groove length. All dimensions are given in mm.

### 2.3. Characterization

For determination of static fracture toughness,  $K_{IC}$ , TDCB specimen was pin loaded and tested with a Hounsfield 10K-S universal testing machine at a crosshead speed of 0.3 mm/min at room temperature (25 °C). Then, the Equation (1) was used for the calculation [46]:

$$K_{IC} = \sqrt{G_{IC}E} = 2P_C \sqrt{\frac{m}{b_n b}} \quad (1)$$

where  $m$  (0.60 mm<sup>-1</sup>) is a constant related to specimen geometry,  $b$  denotes specimen thickness,  $b_n$  is the crack width, and  $P_C$  is the peak force.

Autonomous healing behavior of the TDCB specimens under cyclic stress was evaluated by fatigue test using a Shimadzu air servo fatigue and endurance testing system ADT-AV02K1S5 with 2 kN load cell at 25 °C. The specimens were pre-cracked (~2.5 mm long) by a razor blade, and the pre-crack tip was ensured to be centered in the groove. The specimen was loaded cyclically immediately after the removal of the blade. A triangular waveform of 5 Hz was applied with a stress ratio,  $R$ , of 0.1 ( $R = K_{min}/K_{max}$ , where  $K_{min}$  and  $K_{max}$  denote the minimum and maximum values of the cyclic stress intensity, respectively). Fatigue cracks were grown within constant mode-I stress intensity factor range,  $\Delta K_I$  ( $\Delta K_I = K_{min} - K_{max}$ ). Five specimens were tested for each test when measuring static fracture toughness and cycles to failure. The optically measured crack tip position and specimen compliance were plotted against number of cycles. The linear relationship between optically measured crack length and specimen compliance was used to calculate the crack tip position of the specimens

at all times during the experiment [36]. Healing efficiency,  $\lambda$ , was defined by fatigue life extension [37]:  $\lambda = (N_{healed} - N_{control})/N_{control}$ , where  $N_{healed}$  and  $N_{control}$  denote the total number of cycles to failure of the healed specimen and that of the control specimen without healing, respectively.

Fracture surfaces were observed by a Hitachi Model S-4800 field emission scanning electron microscope (SEM).

## 3. Results and discussion

### 3.1. Effect of the embedded healing capsules on toughness and fatigue life of epoxy composite

Incorporation of fluidic healing agent capsules into epoxy would significantly improve its fatigue performance by increasing the fracture toughness and hence extending the fatigue life [35–38]. Here in this work, the presence of microencapsulated healing agent has also raised the virgin monotonic fracture toughness of epoxy within a wide content range of the capsules. As shown in Figure 2a, when the proportion of epoxy-loaded capsules is less than 6 wt%,  $K_{IC}$  of the composite increases with a rise in the capsules concentration. Even when the content of epoxy-loaded capsules exceeds 10 wt%,  $K_{IC}$  of the composite starts to decrease but is still higher than that of unfilled epoxy until 14 wt%. The results imply that the microcapsules must be well bonded to the matrix [47], so that different fracture mechanisms than voids or solid particles are induced. Compared with the mirror-like fractured surface of unfilled epoxy (Figure 3a), that represents low resistance to crack propagation, the capsules-filled epoxy composite exhibits

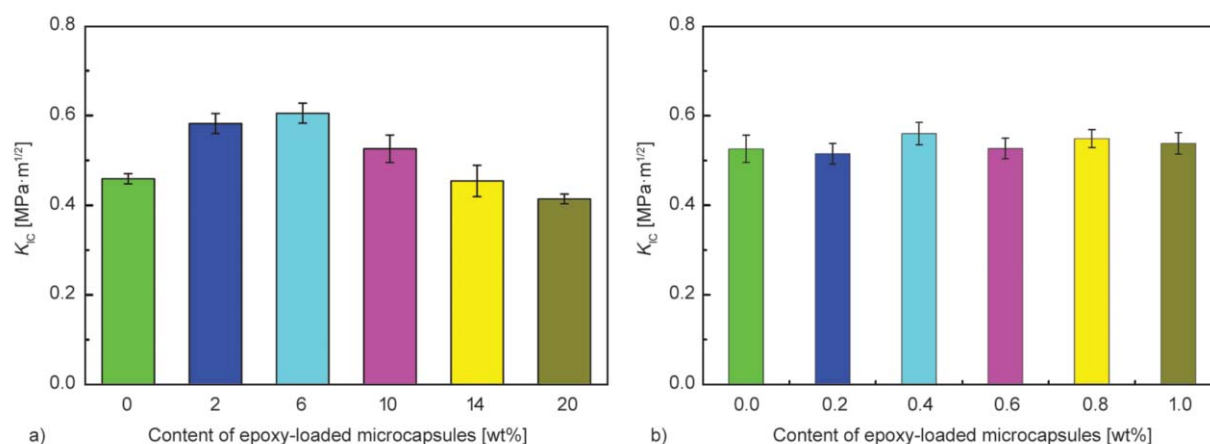


**Figure 2.**  $K_{IC}$  of epoxy composites as a function of (a) content of epoxy-loaded microcapsules and (b) content of hardener-loaded microcapsules. The dosage of hardener-loaded microcapsules is 0 in (a), while that of epoxy-loaded microcapsules is fixed at 10 wt% in (b).

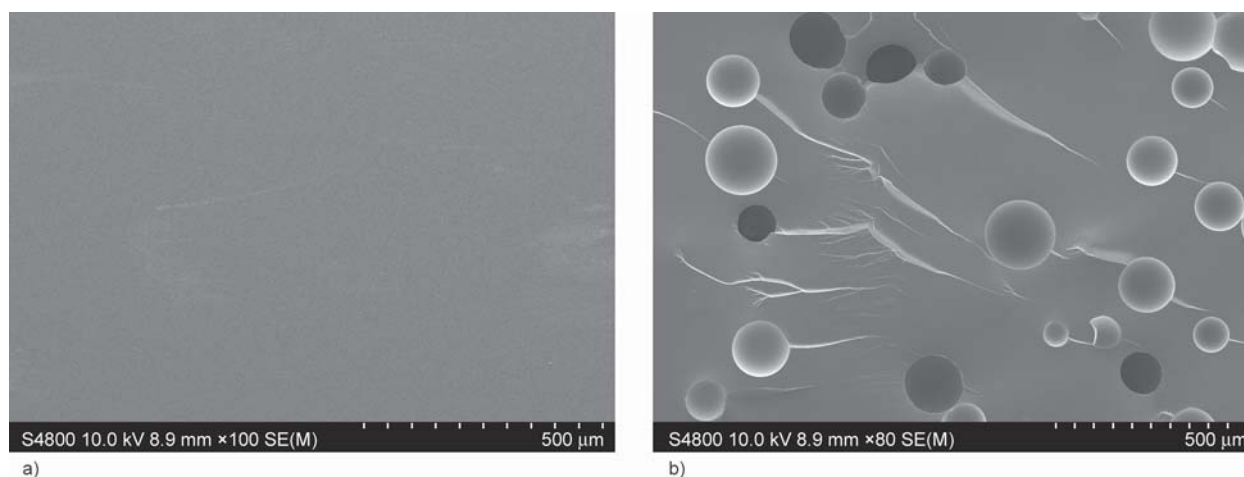


**Figure 3.** SEM micrographs of fracture surfaces of (a) unfilled epoxy and (b) epoxy composite filled with 10 wt% epoxy-loaded microcapsules. Cracks propagate from left to right in the images.

L1 tails structures resulting from crack pinning and  
L2 crack deflection [48] (Figure 3b). Such an out-of-  
L3 plane divergence of cracking consumes more energy  
L4 and hence offers higher fracture toughness.

L5 Although the increment of fracture toughness is not  
L6 significant enough, as characterized by the highest  
L7 increment of 14.6%, the value is comparable to those  
L8 of other self-healing epoxy composites containing  
L9 dual capsules (e.g., 20.2% [38], and 35.3% [49]).

L10 It is known that, the content of healing agent micro-  
L11 capsules must be neither too high nor too low [17].  
L12 The mechanical properties would be deteriorated  
L13 when the dosage is too high, while the healing agent  
L14 (released from the broken capsules) cannot cover the  
L15 crack plane if the dosage is scarce. According to our  
L16 study of recovery of impact strength as a function of  
L17 healing agent concentration of the same self-healing  
L18 composite, content of the epoxy-loaded microcap-  
L19 sules is fixed at 10 wt% hereinafter, so as to supply  
L20 enough healing agent to fill the fatigue crack and  
L21 toughen the epoxy composite as well.

L22 Figure 2b reveals the influence of hardener  
L23 ( $\text{SbF}_5 \cdot \text{HOC}_2\text{H}_5/\text{HOC}_2\text{H}_5$ )-loaded microcapsules on  
L24 fracture toughness of the composite. Because the  
L25 curing of epoxy catalyzed by  $\text{SbF}_5$  follows the mech-  
L26 anism of cationic chain polymerization [27, 28], only  
L27 small amount of the hardener is sufficient to ignite  
L28 the reaction. The stoichiometric ratio of the reaction  
L29 components required by addition polymerization  
L30 [44] is no longer necessary so long as the hardener  
L31 content exceeds a certain critical value, which is an  
L32 advantage of the present healing system. According-  
L33 ly, the loading of the hardener capsules varies below  
L34 1.0 wt%. It is clear that  $K_{IC}$  of the composite nearly  
L35 does not change within the range of interests, as the

contents of the hardener capsules ( $\leq 1.0$  wt%) are  
much lower than that of the epoxy-loaded microcap-  
sules (10 wt%).

Although the hardener-loaded capsules seem to be  
negligible as a toughening agent when appearing to-  
gether with epoxy-loaded microcapsules, they play an  
important role in healing cracks by curing the epoxy  
monomer released from the broken epoxy-loaded  
capsules in the crack tip region during fatigue tests  
[30]. It is seen from Figure 4 that with increasing  
dosage of the hardener-loaded microcapsules, fati-  
gue life of the self-healing composites increases  
firstly and then decreases. This is mainly due to the  
fact that at the beginning the small amount of hard-  
ener-loaded microspheres fails to provide enough  
curing agent for polymerization, leading to incom-  
plete curing of the liberated epoxy. In the case of high

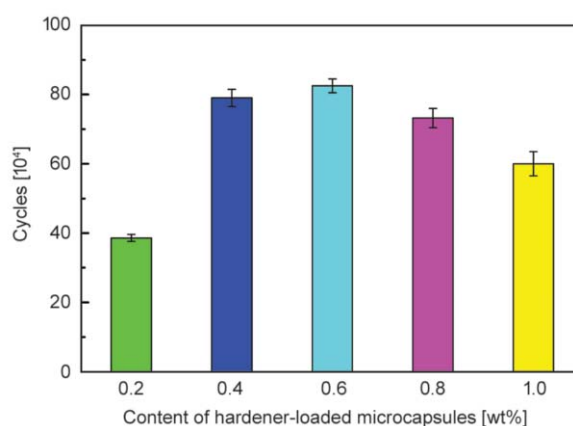


**Figure 4.** Cycles to failure of self-healing epoxy composites vs. content of hardener-loaded microcapsules. Content of epoxy-loaded microcapsules is fixed at 10 wt%. Testing conditions:  $K_{\max} = 0.258 \text{ MPa} \cdot \text{m}^{1/2}$ ,  $K_{\min} = 0.026 \text{ MPa} \cdot \text{m}^{1/2}$ ,  $\Delta K_I = 0.232 \text{ MPa} \cdot \text{m}^{1/2}$ ,  $f = 5 \text{ Hz}$ ,  $R = 0.1$ .

loading of hardener microspheres, higher amount of ethanol included in the excessive hardener ( $\text{SbF}_5 \cdot \text{HOC}_2\text{H}_5/\text{HOC}_2\text{H}_5$ ) may produce defects as stress concentration sites in the wedge formed by the cured healing agent. Fatigue life of the composite has to be shortened as a result of the decreased resistance to fatigue crack growth [35]. In this context, the intermediate content of 0.6 wt%, which corresponds to the highest cycle to failure, is chosen as the optimal proportion. Under the circumstances, adequate hardener is guaranteed to quickly and completely cure the released epoxy monomer, without generating remarkable defects in the polymeric wedge.

### 3.2. Fast self-healing process revealed by fatigue tests

Development of fatigue crack driven by cyclic stress of the related materials is depicted in Figure 5. To rule out the effects of microcapsules toughening and possible hydrodynamic pressure crack-tip shielding of the released healing fluids (an effect of viscous flow within a fatigue crack that decreases the effective range of stress intensity and reduces fatigue crack growth rate [36, 37]), the plot of the control composite containing epoxy- and ethanol-loaded microspheres is also given together with those of unfilled epoxy and self-healing epoxy composite. Relatively speaking, the slope of the dependence of crack length on fatigue cycle of the self-healing specimen (curve 3) is much more gradual, which means that its fatigue life is greatly extended. In the course of fatigue crack growth, the embedded microcapsules in the crack tip are successively ruptured, releasing the healing agent into the crack plane as proved by Figure 6. Accordingly, hydrodynamic pressure crack tip shielding takes effect, as the case of the control specimen (curve 2)

where no reaction could occur. Therefore, fatigue life of the control specimen is about 66.7% higher than that of the unfilled epoxy specimen. It is interesting to see when the released healing agent is allowed to be quickly cured to build up a restoration agent membrane at crack tip to provide effects of cured wedge and adhesive bonding, fatigue crack can be more efficiently retarded as a result of significantly reduced effective stress intensity factor range,  $\Delta K_{\text{eff}}$  ( $\Delta K_{\text{eff}} = \Delta K_I - \Delta K_{\text{toughening}} - \Delta K_{\text{liquid}} - \Delta K_{\text{bonding}} - \Delta K_{\text{wedge}}$ , where  $\Delta K_{\text{toughening}}$  is the stress intensity due to microcapsules induced increase of matrix ductility,  $\Delta K_{\text{liquid}}$  the crack-opening and crack-closure stress intensity from viscosity resistance of the liquid,  $\Delta K_{\text{bonding}}$  the stress intensity due to the combined (tensile) stresses in adhesives across the crack faces, and  $\Delta K_{\text{wedge}}$  the crack-closure stress intensity due to the wedge from adhesives gelling and hardening [38]. The lower  $\Delta K_{\text{eff}}$  implies smaller driving force for the crack growth and hence longer fatigue life). In this case, extension of fatigue crack is further slowed down and fatigue life of the self-healing composite is 282 and 537% longer than those of the control and unfilled epoxy specimens, respectively.

It is worth noting that, the initial slope of curve 3 in Figure 5 is lower than that of the latter part. That is because large amount of healing agent is released and cured when the pre-crack ( $\sim 2.5$  mm long) is made. Comparatively, the quantity of the healing agent subsequently released due to cyclic stress and fatigue crack extension is much smaller. The effects of cured wedge and adhesive bonding of the healing agent in the latter stage are thus less remarkable than those in the initial stage. Nevertheless, the fractographs in Figure 6 demonstrate that the cured membrane generated by the released healing agent

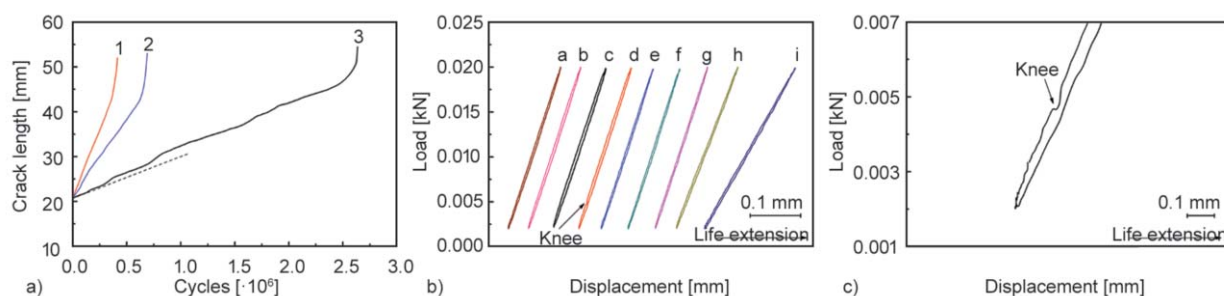


**Figure 5.** (a) Crack length versus fatigue cycle of (1) unfilled epoxy, (2) control and (3) self-healing epoxy composite. (b) Load-displacement curves of self-healing epoxy composite measured during selected cycles in (a). The times counted from starting of fatigue test are shown on top of the corresponding curves. (c) Enlarged view of the curve at 20 seconds in (b) showing the knee phenomenon. Testing conditions:  $K_{\text{max}} = 0.224 \text{ MPa} \cdot \text{m}^{1/2}$ ,  $K_{\text{min}} = 0.022 \text{ MPa} \cdot \text{m}^{1/2}$ ,  $\Delta K_I = 0.202 \text{ MPa} \cdot \text{m}^{1/2}$ ,  $f = 5 \text{ Hz}$ ,  $R = 0.1$ .

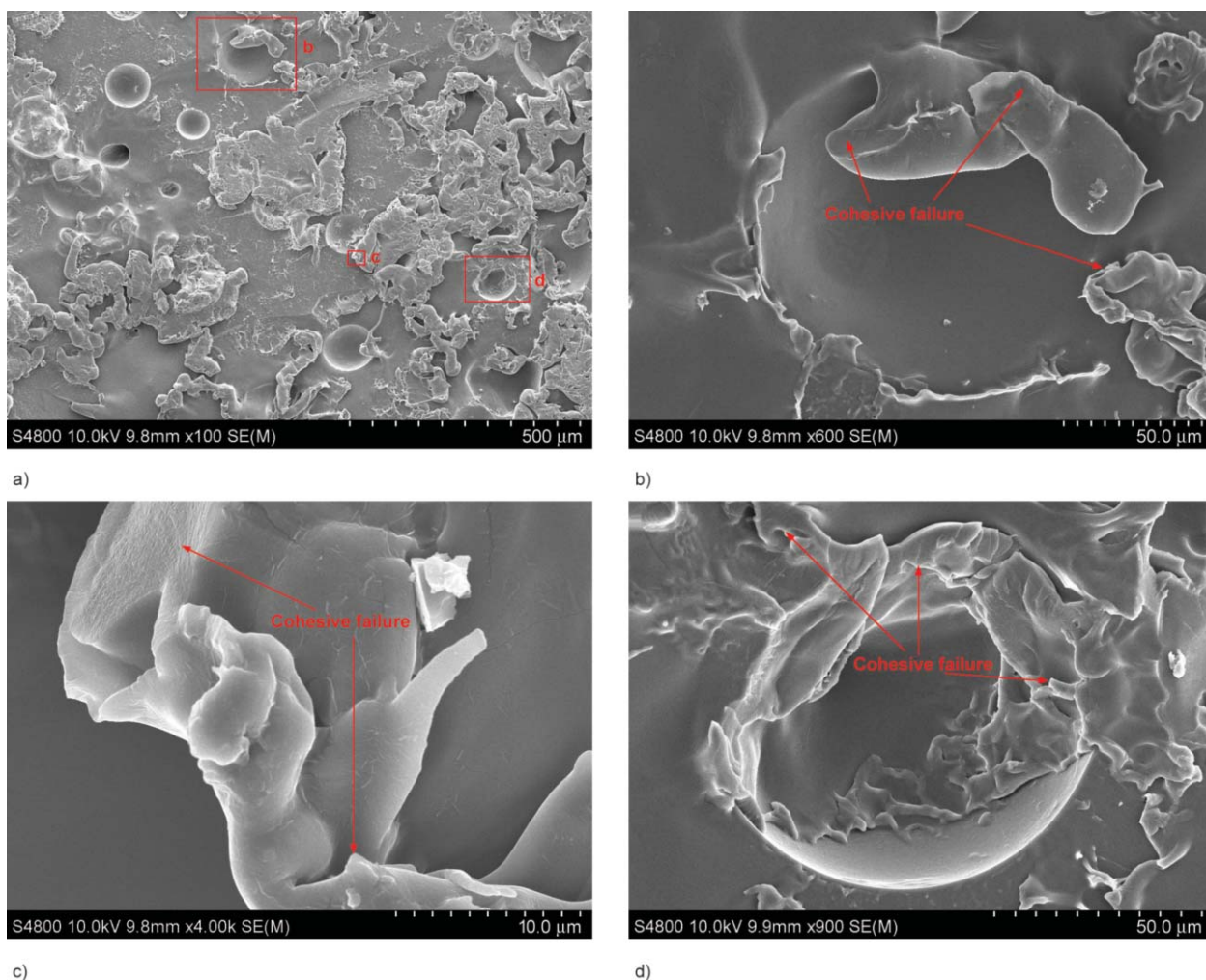


**Figure 6.** SEM micrographs of fatigue fracture surfaces of the self-healing epoxy composite. Testing conditions:  $K_{\max} = 0.224 \text{ MPa} \cdot \text{m}^{1/2}$ ,  $K_{\min} = 0.022 \text{ MPa} \cdot \text{m}^{1/2}$ ,  $\Delta K_I = 0.202 \text{ MPa} \cdot \text{m}^{1/2}$ ,  $f = 5 \text{ Hz}$ ,  $R = 0.1$ .

can well cover the crack surfaces. Accompanying cohesive failure of the healing membranes, fatigue crack gradually passes through the polymeric wedge. Moreover, the remains of the broken wedge still adhere to the cracked plane and decrease the effective stress intensity factor range at the crack tip.

Although the variation in the slope of crack length versus fatigue cycle can sensitively reflect the change of the amount of the healing agent and its performance, we still cannot determine when the healing starts. To look into the details of the self-healing process, load versus displacement of the self-healing epoxy composite is analyzed. As shown in Figure 5b and Figure 5c, a knee point or a deflection appears about 20 seconds as the fatigue test begins. Evidently, the healing agent in the crack plane is converted to solid polymeric wedge as of this time. The deduction coincides with the results of the same healing system introduced to the fatigue crack tip of unfilled epoxy specimen in terms of manual infiltration [30]. Therefore,

the time at which a knee point is observed on the dependence of load on displacement can be regarded as the onset time of self-healing. Comparatively, the measurable healing of other systems used to be first observed couple of minutes or even longer time after the tests started [24–28, 44, 46, 50]. It means that the present healing agent can offer much faster healing.

### 3.3. Effect of $\Delta K_I$ on self-healing efficiency

Owing to the configuration of fatigue test, the measured self-healing efficiency is closely dependent on the applied stress intensity factor,  $\Delta K_I$ , in addition to the polymerization rate of embedded healing agent. In the following, fatigue performance of the self-healing epoxy composite measured at three  $\Delta K_I$  values is discussed.

As shown in Figure 7a and Figure 7b, the repairing efficiencies tested at higher  $\Delta K_I$  values ( $0.252$  and  $0.232 \text{ MPa} \cdot \text{m}^{1/2}$ ) are 64.9 and 167%, respectively. In these cases, mechanical kinetics of crack propagation

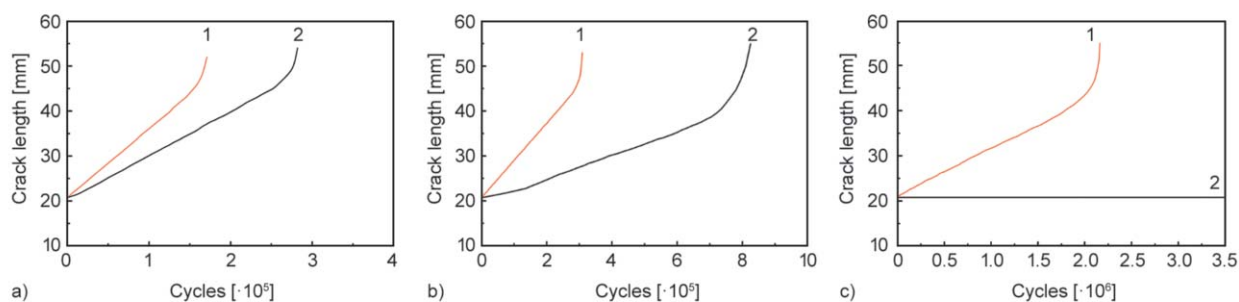


**Figure 7.** Crack length vs. fatigue cycles of (1) control and (2) self-healing epoxy composite. Testing conditions: (a)  $K_{\max} = 0.280 \text{ MPa}\cdot\text{m}^{1/2}$ ,  $K_{\min} = 0.028 \text{ MPa}\cdot\text{m}^{1/2}$ ,  $\Delta K_I = 0.252 \text{ MPa}\cdot\text{m}^{1/2}$ ,  $f = 5 \text{ Hz}$ ,  $R = 0.1$ ; (b)  $K_{\max} = 0.258 \text{ MPa}\cdot\text{m}^{1/2}$ ,  $K_{\min} = 0.026 \text{ MPa}\cdot\text{m}^{1/2}$ ,  $\Delta K_I = 0.232 \text{ MPa}\cdot\text{m}^{1/2}$ ; (c)  $K_{\max} = 0.202 \text{ MPa}\cdot\text{m}^{1/2}$ ,  $K_{\min} = 0.020 \text{ MPa}\cdot\text{m}^{1/2}$ ,  $\Delta K_I = 0.182 \text{ MPa}\cdot\text{m}^{1/2}$ .

predominates so that fatigue crack grows faster. Moreover, the amount of the released healing agent squeezed out of the crack tip would be higher, implying that the effects of hydrodynamic pressure crack tip shielding and adhesive bonding have to be weakened [36, 37]. In the meantime, the polymeric wedge formed at crack tip is easy to be deformed or even destroyed. All these factors go against fatigue life extension.

When  $\Delta K_I$  value is reduced to  $0.182 \text{ MPa}\cdot\text{m}^{1/2}$ , it is interesting to see from Figure 7c that fatigue crack is arrested as chemical kinetics of healing agent plays the leading role. The crack can hardly advance forward within the entire range of measured cycles, which corresponds to infinite healing efficiency. Under the circumstances, fewer healing agent is squeezed out of crack tip, and bigger polymeric wedge can be produced within short time as a result of the fast curing of the healing system. The experiment clearly highlights the significance of healing speed.

Figure 8 summarizes the healing efficiencies measured at different ranges of applied stress intensity factor. When  $\Delta K_I$  is decreased, the fatigue crack retardancy is obviously increased as discussed hereinbefore,

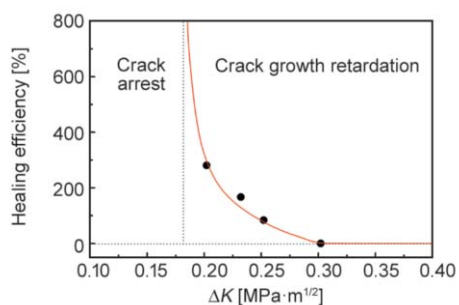


**Figure 8.** Healing efficiency of self-healing epoxy composite as a function of range of applied stress intensity factor. The data are calculated partly using the results in Figure 5a and Figure 7

leading to longer fatigue life. The critical  $\Delta K_I$  value lies in  $0.182 \text{ MPa}\cdot\text{m}^{1/2}$ . For  $\Delta K_I \leq 0.182 \text{ MPa}\cdot\text{m}^{1/2}$ , fatigue crack of the self-healing epoxy composite is fully arrested. Based on this finding, it is known that the critical  $\Delta K_I$  value may act as another measure of healing speed, in addition to the onset healing time estimated from displacement dependence of load (Figure 5). That is, the higher critical  $\Delta K_I$  value suggests the faster the healing reaction. It reflects the ultimate effect of healing agent, and may be more meaningful than the onset healing time when comparing chemical kinetics of different self-healing agents working for the same polymer (i.e. the polymer to be repaired).

#### 4. Conclusions

Self-healing epoxy composite filled with microencapsulated epoxy monomer and  $\text{SbF}_5 \text{ HOC}_2\text{H}_5/\text{HOC}_2\text{H}_5$  proves to be able to retard or arrest fatigue crack growth. The beneficial effects of the microcapsules are embodied in the form of intact fluid-loaded spheres, released fluidic healing agent, and solidified version of the healing agent. Firstly, the embedded microcapsules toughen the epoxy matrix. Then, the crack induces breakage of the healing capsules, and the liberated fluidic healing agent hinders the advancement of crack via hydrodynamic pressure crack tip shielding. Finally, the released healing agent is polymerized forming polymeric wedge and adhesive bonding, both of which obstruct crack propagation. Because the curing of the healing system proceeds very fast, the healing represented by the generation of solid wedge is detected only 20 seconds after start of the fatigue test. In this context, the healing agent developed in this work possesses the application potential for autonomic fast restoration of polymer products.

## Acknowledgements

The authors thank the support from the Natural Science Foundation of China (Grants: 51333008 and 51673219), the Natural Science Foundation of Guangdong (Grants: 2010B010800021 and S2013020013029), and the Science and Technology Program of Guangzhou (Grants: 2014J4100121 and 201604010105).

## References

- [1] Zhang M. Q., Rong M. Z.: Self-healing polymers and polymer composites. Wiley, Hoboken (2011).
- [2] Yuan Y. C., Yin T., Rong M. Z., Zhang M. Q.: Self healing in polymers and polymer composites. Concepts, realization and outlook: A review. *Express Polymer Letters*, **2**, 238–250 (2008).  
<https://doi.org/10.3144/expresspolymlett.2008.29>
- [3] Binder W. H.: Self-healing polymers. Wiley-VCH, Weinheim (2013).
- [4] Wu S. W., Li J. H., Zhang G. P., Yao Y. M., Li G., Sun R., Wong C. P.: Ultrafast self-healing nanocomposites via infrared laser and their application in flexible electronics. *ACS Applied Materials and Interfaces*, **9**, 3040–3049 (2017).  
<https://doi.org/10.1021/acsami.6b15476>
- [5] Cordier P., Tournilhac F., Soulie-Ziakovic C., Leibler L.: Self-healing and thermoreversible rubber from supramolecular assembly. *Nature*, **451**, 977–980 (2008).  
<https://doi.org/10.1038/nature06669>
- [6] Burattini S., Colquhoun H. M., Fox J. D., Friedmann D., Greenland B. W., Harris P. J. F., Hayes W., Mackay M. E., Rowan S. J.: A self-repairing, supramolecular polymer system: Healability as a consequence of donor-acceptor  $\pi$ - $\pi$  stacking interactions. *Chemical Communications*, 2009, 6717–6719 (2009).  
<https://doi.org/10.1039/b910648k>
- [7] Varley R. J., van der Zwaag S.: Autonomous damage initiated healing in a thermo-responsive ionomer. *Polymer International*, **59**, 1031–1038 (2010).  
<https://doi.org/10.1002/pi.2841>
- [8] Nakahata M., Takashima Y., Yamaguchi H., Harada A.: Redox-responsive self-healing materials formed from host-guest polymers. *Nature Communications*, **2**, 511/1–511/6 (2011).  
<https://doi.org/10.1038/ncomms1521>
- [9] Xia N. N., Xiong X. M., Wang J., Rong M. Z., Zhang M. Q.: A seawater triggered dynamic coordinate bond and its application for underwater self-healing and reclaiming of lipophilic polymer. *Chemical Science*, **7**, 2736–2742 (2016).  
<https://doi.org/10.1039/c5sc03483c>
- [10] Roy N., Buhler E., Lehn J-M.: Double dynamic self-healing polymers: Supramolecular and covalent dynamic polymers based on the bis-iminocarbohydrazide motif. *Polymer International*, **63**, 1400–1405 (2014).  
<https://doi.org/10.1002/pi.4646>
- [11] Lei Z. Q., Xie P., Rong M. Z., Zhang M. Q.: Catalyst-free dynamic exchange of aromatic Schiff base bonds and its application to self-healing and remolding of crosslinked polymers. *Journal of Materials Chemistry A*, **3**, 19662–19668 (2015).  
<https://doi.org/10.1039/c5ta05788d>
- [12] Chen X., Dam M. A., Ono K., Mal A., Shen H., Nutt S. R., Sheran K., Wudl F.: A thermally re-mendable cross-linked polymeric material. *Science*, **295**, 1698–1702 (2002).  
<https://doi.org/10.1126/science.1065879>
- [13] Xiang H. P., Qian H. J., Lu Z. Y., Rong M. Z., Zhang M. Q.: Crack healing and reclaiming of vulcanized rubber by triggering the rearrangement of inherent sulfur crosslinked networks. *Green Chemistry*, **17**, 4315–4325 (2015).  
<https://doi.org/10.1039/c5gc00754b>
- [14] Zhang Z. P., Rong M. Z., Zhang M. Q., Yuan C. E.: Alkoxyamine with reduced homolysis temperature and its application in repeated autonomous self-healing of stiff polymers. *Polymer Chemistry*, **4**, 4648–4654 (2013).  
<https://doi.org/10.1039/c3py00679d>
- [15] Ling J., Rong M. Z., Zhang M. Q.: Effect of molecular weight of PEG soft segments on photo-stimulated self-healing performance of coumarin functionalized polyurethanes. *Chinese Journal of Polymer Science*, **32**, 1286–1297 (2014).  
<https://doi.org/10.1007/s10118-014-1522-x>
- [16] Xia N. N., Rong M. Z., Zhang M. Q.: Stabilization of catechol–boronic ester bonds for underwater self-healing and recycling of lipophilic bulk polymer in wider pH range. *Journal of Materials Chemistry A*, **4**, 14122–14131 (2016).  
<https://doi.org/10.1039/c6ta05121a>
- [17] Zhu D. Y., Rong M. Z., Zhang M. Q.: Self-healing polymeric materials based on microencapsulated healing agents: From design to preparation. *Progress in Polymer Science*, **49–50**, 175–220 (2015).  
<https://doi.org/10.1016/j.progpolymsci.2015.07.002>
- [18] Vijayan P., AlMaadeed M. A.: ‘Containers’ for self-healing epoxy composites and coating: Trends and advances. *Express Polymer Letters*, **10**, 506–524 (2016).  
<https://doi.org/10.3144/expresspolymlett.2016.48>
- [19] Luterbacher R., Coope T. S., Trask R. S., Bond I. P.: Vascular self-healing within carbon fibre reinforced polymer stringer run-out configurations. *Composites Science and Technology*, **136**, 67–75 (2016).  
<https://doi.org/10.1016/j.compscitech.2016.10.007>
- [20] Zhu Y., Ye X. J., Rong M. Z., Zhang M. Q.: Self-healing glass fiber/epoxy composites with polypropylene tubes containing self-pressurized epoxy and mercaptan healing agents. *Composites Science and Technology*, **135**, 146–152 (2016).  
<https://doi.org/10.1016/j.compscitech.2016.09.020>

- [21] Szebényi G., Czigány T., Vermes B., Ye X. J., Rong M. Z., Zhang M. Q.: Acoustic emission study of the TDCB test of microcapsules filled self-healing polymer. *Polymer Testing*, **54**, 134–138 (2016).  
<https://doi.org/10.1016/j.polymertesting.2016.07.005>
- [22] Billiet S., Hillewaere X. K., Teixeira R. F., Du Prez F. E.: Chemistry of crosslinking processes for self-healing polymers. *Macromolecular Rapid Communication*, **34**, 290–309 (2013).  
<https://doi.org/10.1002/marc.201200689>
- [23] Yi H., Deng Y., Wang C.: Pickering emulsion-based fabrication of epoxy and amine microcapsules for dual core self-healing coating. *Composites Science and Technology*, **133**, 51–59 (2016).  
<https://doi.org/10.1016/j.compscitech.2016.07.022>
- [24] Cao G. S., Rong M. Z., Zhang M. Q., Ye X. J.: Self-healing of thermally molded commodity plastics based on heat-resistant and anti-aging healing systems. *RSC Advances*, **6**, 93410–93418 (2016).  
<https://doi.org/10.1039/C6RA18485E>
- [25] Li C., Tan J., Gu J., Qiao L., Zhang B., Zhang Q.: Rapid and efficient synthesis of isocyanate microcapsules *via* thiol-ene photopolymerization in Pickering emulsion and its application in self-healing coating. *Composites Science and Technology*, **123**, 250–258 (2016).  
<https://doi.org/10.1016/j.compscitech.2016.01.001>
- [26] Zhu D. Y., Guo J. W., Cao G. S., Qiu W. L., Rong M. Z., Zhang M. Q.: Thermo-moldable self-healing commodity plastics with heat resisting and oxygen-insensitive healant capable of room temperature redox cationic polymerization. *Journal of Materials Chemistry A*, **3**, 1858–1862 (2015).  
<https://doi.org/10.1039/C4TA06381C>
- [27] Xiao D. S., Yuan Y. C., Rong M. Z., Zhang M. Q.: A facile strategy for preparing self-healing polymer composites by incorporation of cationic catalyst-loaded vegetable fibers. *Advanced Functional Materials*, **19**, 2289–2296 (2009).  
<https://doi.org/10.1002/adfm.200801827>
- [28] Xiao D. S., Yuan Y. C., Rong M. Z., Zhang M. Q.: Hollow polymeric microcapsules: Preparation, characterization and application in holding boron trifluoride diethyl etherate. *Polymer*, **50**, 560–568 (2009).  
<https://doi.org/10.1016/j.polymer.2008.11.022>
- [29] Ye X. J., Zhang J-L., Zhu Y., Rong M. Z., Zhang M. Q., Song Y. X., Zhang H-X.: Ultrafast self-healing of polymer toward strength restoration. *ACS Applied Materials and Interfaces*, **6**, 3661–3670 (2014).  
<https://doi.org/10.1021/am405989b>
- [30] Ye X. J., Zhu Y., Yuan Y. C., Song Y. X., Yang G. C., Rong M. Z., Zhang M. Q.: Fatigue life extension of epoxy materials using ultrafast epoxy-SbF<sub>5</sub> healing system introduced by manual infiltration. *Express Polymer Letters*, **9**, 177–184 (2015).  
<https://doi.org/10.3144/expresspolymlett.2015.19>
- [31] Zhang M. Q.: Polymer self-heals in seconds. *Express Polymer Letters*, **9**, 84 (2015).  
<https://doi.org/10.3144/expresspolymlett.2015.9>
- [32] Ye X. J., Song Y. X., Zhu Y., Yang G. C., Rong M. Z., Zhang M. Q.: Self-healing epoxy with ultrafast and heat-resistant healing system processable at elevated temperature. *Composites Science and Technology*, **104**, 40–46 (2014).  
<https://doi.org/10.1016/j.compscitech.2014.08.028>
- [33] Song Y. X., Ye X. J., Rong M. Z., Zhang M. Q.: Self-healing epoxy with a fast and stable extrinsic healing system based on BF<sub>3</sub>-amine complex. *RSC Advances*, **6**, 100796–100803 (2016).  
<https://doi.org/10.1039/C6RA17976B>
- [34] Jones A. S., Rule J. D., Moore J. S., Sottos N. R., White S. R.: Life extension of self-healing polymers with rapidly growing fatigue cracks. *Journal of the Royal Society Interface*, **4**, 395–403 (2007).  
<https://doi.org/10.1098/rsif.2006.0199>
- [35] Yuan Y. C., Rong M. Z., Zhang M. Q., Yang G. C., Zhao J. Q.: Healing of fatigue crack in epoxy materials with epoxy/mercaptan system *via* manual infiltration. *Express Polymer Letters*, **4**, 644–658 (2010).  
<https://doi.org/10.3144/expresspolymlett.2010.79>
- [36] Brown E. N., White S. R., Sottos N. R.: Retardation and repair of fatigue cracks in a microcapsule toughened epoxy composite – Part II: *In situ* self-healing. *Composites Science and Technology*, **65**, 2474–2480 (2005).  
<https://doi.org/10.1016/j.compscitech.2005.04.053>
- [37] Brown E. N., White S. R., Sottos N. R.: Retardation and repair of fatigue cracks in a microcapsule toughened epoxy composite – Part I: Manual infiltration. *Composites Science and Technology*, **65**, 2466–2473 (2005).  
<https://doi.org/10.1016/j.compscitech.2005.04.020>
- [38] Yuan Y. C., Rong M. Z., Zhang M. Q., Yang G. C., Zhao J. Q.: Self-healing of fatigue crack in epoxy materials with epoxy/mercaptan system. *Express Polymer Letters*, **5**, 47–59 (2011).  
<https://doi.org/10.3144/expresspolymlett.2011.6>
- [39] Pingkarawat K., Wang C. H., Varley R. J., Mouritz A. P.: Self-healing of delamination fatigue cracks in carbon fibre-epoxy laminate using mendable thermoplastic. *Journal of Materials Science*, **47**, 4449–4456 (2012).  
<https://doi.org/10.1007/s10853-012-6303-8>
- [40] Hamilton A. R., Sottos N. R., White S. R.: Mitigation of fatigue damage in self-healing vascular materials. *Polymer*, **53**, 5575–5581 (2012).  
<https://doi.org/10.1016/j.polymer.2012.09.050>
- [41] Neuser S., Michaud V.: Fatigue response of solvent-based self-healing smart materials. *Experimental Mechanics*, **54**, 293–304 (2014).  
<https://doi.org/10.1007/s11340-013-9787-5>
- [42] Luterbacher R., Trask R. S., Bond I. P.: Static and fatigue tensile properties of cross-ply laminates containing vasculs for self-healing applications. *Smart Materials and Structures*, **25**, 015003/1–015003/10 (2016).  
<https://doi.org/10.1088/0964-1726/25/1/015003>

- [43] Lee M. W., Sett S., Yoon S. S., Yarin A. L.: Fatigue of self-healing nanofiber-based composites: Static test and subcritical crack propagation. *ACS Applied Materials and Interfaces*, **8**, 18462–18470 (2016).  
<https://doi.org/10.1021/acsami.6b05390>
- [44] Yuan Y. C., Rong M. Z., Zhang M. Q., Chen J., Yang G. C., Li X. M.: Self-healing polymeric materials using epoxy/mercaptan as the healant. *Macromolecules*, **41**, 5197–5202 (2008).  
<https://doi.org/10.1021/ma800028d>
- [45] Ye X-J., Ma Z-X., Song Y-X., Huang J-J., Rong M-Z., Zhang M-Q.: SbF<sub>5</sub>-loaded microcapsules for ultrafast self-healing of polymer. *Chinese Chemical Letters*, **25**, 1565–1568 (2014).  
<https://doi.org/10.1016/j.cclet.2014.07.002>
- [46] Brown E. N., Sottos N. R., White S. R.: Fracture testing of a self-healing polymer composite. *Experimental Mechanics*, **42**, 372–379 (2002).  
<https://doi.org/10.1007/BF02412141>
- [47] Brown E. N., White S. R., Sottos N. R.: Microcapsule induced toughening in a self-healing polymer composite. *Journal of Materials Science*, **39**, 1703–1710 (2004).  
<https://doi.org/10.1023/B:JMSSC.0000016173.73733.dc>
- [48] Kinloch A. J., Maxwell D. L., Young R. J.: The fracture of hybrid-particulate composites. *Journal of Materials Science*, **20**, 4169–4184 (1985).  
<https://doi.org/10.1007/BF00552413>
- [49] Yuan Y. C., Ye X. J., Rong M. Z., Zhang M. Q., Yang G. C., Zhao J. Q.: Self-healing epoxy composite with heat-resistant healant. *ACS Applied Materials and Interfaces*, **3**, 4487–4495 (2011).  
<https://doi.org/10.1021/am201182j>
- [50] Mauldin T. C., Rule J. D., Sottos N. R., White S. R., Moore J. S.: Self-healing kinetics and the stereoisomers of dicyclopentadiene. *Journal of The Royal Society Interface*, **4**, 389–393 (2007).  
<https://doi.org/10.1098/rsif.2006.0200>